

**Response to interactive comment on “Nitrate formation from heterogeneous uptake of dinitrogen pentoxide during a severe winter haze in southern China” by Hui Yun et al. from anonymous Referee #1**

**The reviewers’ comments are italicized followed by our responses and changes in manuscript shown in blue and red, respectively. And the corrections are also marked as red color in the revised manuscript.**

*The manuscript of Yun et al., reported half month measurement of  $N_2O_5$ ,  $ClNO_2$  and other relative parameters during heavy haze episodes in Pearl River Delta (PRD) of southern China. The  $N_2O_5$  uptake coefficient and  $ClNO_2$  yield were determined from the observations. The study showed the observation evidence of the enhancement of particulate nitrate in the first several hours can be fully explained by the  $N_2O_5$  heterogeneous hydrolysis and even comparable with the nitric acid formed by  $OH+NO_2$  during daytime. Overall, the paper contributes to the knowledge of  $N_2O_5$  heterogeneous chemistry and highlight the heterogeneous reactions in the formation of particulate nitrate in southern China. The following comments should be addressed before publishing on ACP.*

**Response:** We appreciate the reviewer for the positive comments which are addressed in detail below.

**Major comments:**

*The steady state assumption to derive the  $N_2O_5$  uptake coefficient needs to be verified by model simulations under the observed conditions (with input from  $NO$ ,  $NO_2$ ,  $O_3$ , VOCs). It is useful to try other method (e.g. Brown et al., 2006) to derive  $N_2O_5$  uptake coefficient.*

*Brown, S. S., Ryerson, T. B., Wollny, A. G., Brock, C. A., Peltier, R., Sullivan, A. P., Weber, R. J., Dube, W. P., Trainer, M., Meagher, J. F., Fehsenfeld, F. C., and Ravishankara, A. R.: Variability in nocturnal nitrogen oxide processing and its role in regional air quality, *Science*, 311, 67-70, DOI 10.1126/science.1120120, 2006.*

**Response:** The method used to derive the  $N_2O_5$  uptake coefficient in our manuscript did not require an assumption of  $NO_3$  radical being in steady state, but assumed that the change of

$\text{NO}_3$  and  $\text{N}_2\text{O}_5$  concentrations was mainly caused by  $\text{NO}_3/\text{N}_2\text{O}_5$  chemistry. The value of  $\frac{d([\text{N}_2\text{O}_5]+[\text{NO}_3])}{dt}$  was not required to be nearly zero as the method of Brown et al., 2006, but was calculated with the measured concentration of  $\text{N}_2\text{O}_5$  and the calculated concentration of  $\text{NO}_3$ . We believe our method allows more data for use in analysis than the steady-state approach.

Indeed we compare our method with the steady-state approximation (Brown et al., 2006) for calculation of the  $\gamma_{\text{N}_2\text{O}_5}$  using equation (1) below. The plots of  $\tau_{\text{N}_2\text{O}_5}^{-1}\text{K}_{\text{eq}}[\text{NO}_2]$  correlated to  $0.25c_{\text{N}_2\text{O}_5}\text{SaK}_{\text{eq}}[\text{NO}_2]$  for four selected air masses in short-time periods which were proper to use the steady state assumption are presented in Figure 1 here. The  $\gamma_{\text{N}_2\text{O}_5\text{-steady-state}}$  varied from 0.008 to 0.012 and was comparable to the uptake coefficients derived with the method in the manuscript in the same periods (see Table 1 here).

$$(1) \tau_{\text{N}_2\text{O}_5}^{-1}K_{\text{eq}}[\text{NO}_2] \approx k_g + \frac{1}{4}C_{\text{N}_2\text{O}_5} \text{Sa} \gamma_{\text{N}_2\text{O}_5} K_{\text{eq}}[\text{NO}_2]$$

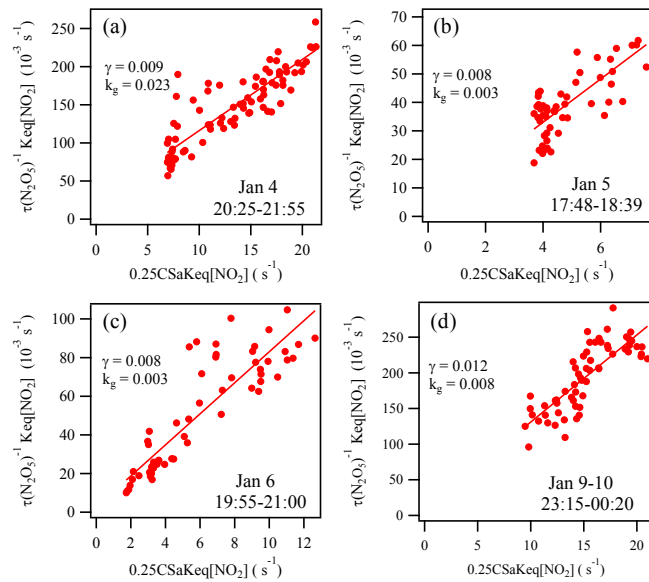


Figure 1. Plots of  $\tau_{\text{N}_2\text{O}_5}^{-1}\text{K}_{\text{eq}}[\text{NO}_2]$  versus  $0.25c_{\text{N}_2\text{O}_5}\text{SaK}_{\text{eq}}[\text{NO}_2]$  for selected air masses.

Table 1. Comparison of  $\gamma_{N_2O_5}$  derived with steady state method and with the method in the manuscript in the same periods.

Date	$\gamma_{N_2O_5}$ -steady-state	$\gamma_{N_2O_5}$ in the manuscript
Jan 4 20:26-21:56	0.009	0.011
Jan 5 17:48-18:39	0.008	0.007
Jan 6 19:55-21:00	0.008	0.009
Jan 9 23:15-00:20	0.012	0.014

Without the need for steady-state assumption, we can make use of more observation data to derive the updated parameters.

*The uncertainty of the measured  $N_2O_5$ , NMHC and Sa and the overall uncertainty propagated to  $N_2O_5$  uptake coefficient and  $ClNO_2$  yield should be carefully evaluated and discussed. As the hygroscopic growth factor is hard to quantify for RH over 90%, the derived  $N_2O_5$  uptake coefficient for those conditions may subject with larger uncertainties compared with other RH cases. This is an interesting point to be discussed.*

Response: The uncertainty of the measured  $N_2O_5$  and NMHC was  $\pm 25\%$  and  $\pm 20\%$ , respectively, which will influence the item of  $\frac{k_{NO_2+O_3}[NO_2][O_3]}{[N_2O_5]}$  and  $\frac{\sum k_i[VOC_i]}{[NO_2] \times K_{eq}}$  in equation (2) here. According to the calculation in our manuscript,  $k'_{N_2O_5}$  was two orders of magnitude higher than that of  $\frac{\sum k_i[VOC_i]}{[NO_2] \times K_{eq}}$ , suggesting the value of  $\frac{k_{NO_2+O_3}[NO_2][O_3]}{[N_2O_5]}$  was far more than  $\frac{\sum k_i[VOC_i]}{[NO_2] \times K_{eq}}$ . Hence, the uncertainty of  $N_2O_5$  uptake coefficient was mainly caused by the uncertainty of  $N_2O_5$ ,  $NO_2$  ( $\pm 20\%$ ),  $O_3$  ( $\pm 5\%$ ) and  $Sa$ . The hygroscopic growth factor is hard to quantify for RH over 90%, thus the calculated  $Sa$  would present large uncertainty when RH reached over 90%. The average RH ranged from 59-85% during the selected periods in Table 2 in the revised manuscript. The uncertainty of  $Sa$  with RH below 90% was estimated to be around  $\pm 30\%$  (Tham et al., 2016; Wang Z et al., 2017). The uncertainty of the calculated  $N_2O_5$  uptake coefficient was then derived to be  $\pm 45\%$ . The uncertainty of  $ClNO_2$  yield was mainly caused by the uncertainty of  $NO_2$  ( $\pm 20\%$ ),  $O_3$  ( $\pm 5\%$ ) and  $ClNO_2$  ( $\pm 25\%$ ) and was derived to be  $\pm 30\%$ .

$$(2) k'_{N_2O_5} = \frac{k_{NO_2+O_3}[NO_2][O_3]}{[N_2O_5]} - \frac{d[N_2O_5]}{[N_2O_5]dt} - \frac{d(\frac{[N_2O_5]}{[NO_2] \times K_{eq}})}{[N_2O_5]dt} - \frac{\sum k_i[VOC_i]}{[NO_2] \times K_{eq}} = \frac{1}{4} C_{N_2O_5} S_a \gamma_{N_2O_5}$$

Tham, Y. J., Wang, Z., Li, Q., Yun, H., Wang, W., Wang, X., Xue, L., Lu, K., Ma, N., Bohn, B., Li, X., Kecorius, S., Größ, J., Shao, M., Wiedensohler, A., Zhang, Y., and Wang, T.: Significant concentrations of nitril chloride sustained in the morning: investigations of the causes and impacts on ozone production in a polluted region of northern China, *Atmos. Chem. Phys.*, 16, 14959-14977, 10.5194/acp-16-14959-2016, 2016.

Wang, Z., Wang, W., Tham, Y. J., Li, Q., Wang, H., Wen, L., Wang, X., and Wang, T.: Fast heterogeneous  $N_2O_5$  uptake and  $ClNO_2$  production in power plant and industrial plumes observed in the nocturnal residual layer over the North China Plain, *Atmos. Chem. Phys.*, 17, 12361-12378, 10.5194/acp-17-12361-2017, 2017.

In the manuscript, the following sentences were added:

Line 338-341: The uncertainty of the above  $\gamma_{N_2O_5}$  was estimated to be  $\pm 45\%$  due to the measurement uncertainty of  $N_2O_5$  ( $\pm 25\%$ ),  $NO_2$  ( $\pm 20\%$ ),  $O_3$  ( $\pm 5\%$ ) and  $Sa$  ( $\pm 30\%$ ). The uncertainty of  $\phi_{ClNO_2}$  was mainly caused by the uncertainty of  $NO_2$  ( $\pm 20\%$ ),  $O_3$  ( $\pm 5\%$ ) and  $ClNO_2$  ( $\pm 25\%$ ) and was estimated to be  $\pm 30\%$ .

*The relationship between  $N_2O_5$  uptake coefficient,  $ClNO_2$  yield and the chemical properties of particles or the meteorological data (such as RH) should be investigated, especially in the part of text around Line 572 (table 1), the reason of the high gamma value in the Jan.3 17:40-20:50 should be addressed as which was much higher than other derived value.*

Response: We examined the correlation between  $N_2O_5$  uptake coefficient,  $ClNO_2$  yield and the concentrations of aerosol compositions or RH, and the results did not show any significant dependence of uptake coefficient/yield on these parameters. The below Table was added in the SI as Table S2.

Table 2. Average values ( $\mu\text{g m}^{-3}$ ) of  $\text{PM}_{2.5}$  loadings and the composition of  $\text{PM}_{2.5}$  during the time periods corresponding to Table 2 in the revised manuscript.

Date	$\text{Cl}^-$	$\text{NO}_3^-$	$\text{SO}_4^{2-}$	$\text{NH}_4^+$	OM	EC	$\text{PM}_{2.5}$
Jan 3 17:40-19:00	0.9	19.7	8.8	6.5	37.4	8.0	86.4
Jan 4 17:00-22:00	1.5	44.3	8.7	12.0	44.6	13.2	150.7
Jan 5 17:00-22:00	1.6	68.9	15.5	15.3	56.6	14.2	216.6
Jan 6 17:00-22:40	2.7	40.0	15.7	13.8	54.6	10.5	174.3
Jan 9 19:00-00:20	0.8	29.9	7.2	8.9	36.7	11.6	117.3

Regarding the Jan 3rd case, the concentration of  $\text{N}_2\text{O}_5$  and the  $\text{Sa}$  were both the lowest in the five cases, and the  $\text{P}_{\text{NO}_3}$  was the highest among all cases, leading to high  $\text{N}_2\text{O}_5$  uptake coefficient. Taking a closer look at the data of that night, it can be divided into two periods with relatively high  $\text{N}_2\text{O}_5$  of 200 pptv on average from 17:40-19:00 and low  $\text{N}_2\text{O}_5$  of only 15 pptv on average from 19:10-20:50 (see Table 2 below and Figure 2 data in the red box). The second period was influenced more by fresh emission during the transportation of the air mass as indicated by the more variable  $\text{NO}_2$  and  $\text{O}_3$ , making the calculation of  $\gamma_{\text{N}_2\text{O}_5}$  and  $\phi_{\text{CINO}_2}$  more difficult. In the revised manuscript, we decided to drop the second period, and the  $\gamma_{\text{N}_2\text{O}_5}$  was 0.066 (17:40-19:00) in the Jan 3 case.

Table 3. Details for the two parts of the selected period from 17:40-20:50 on the night of Jan 3, 2017.

Date	$\text{N}_2\text{O}_5$ pptv	Max- $\text{CINO}_2$ pptv	$\text{NO}_2$ ppbv	$\text{O}_3$ ppbv	RH %	$\text{Sa}$ $\mu\text{m}^2 \text{cm}^{-3}$	$\text{P}_{\text{NO}_3}$ ppbv $\text{h}^{-1}$	$k_{\text{NO}_3}$ $10^{-3} \text{s}^{-1}$	$L_{\text{N}_2\text{O}_5}$ ppbv $\text{h}^{-1}$	$k_{\text{NO}_3}/(\text{K}_{\text{eq}}[\text{NO}_2])$ $10^{-5} \text{s}^{-1}$	$k_{\text{N}_2\text{O}_5}$ $10^{-3} \text{s}^{-1}$	$\gamma_{\text{N}_2\text{O}_5}$	$\phi_{\text{CINO}_2}$
Jan 3 17:40-19:00	200	1029	20.0	77.8	59	2170	4.3	0.516	4.3	3.03	8.8	0.066	0.18
Jan 3 19:10-20:50	15	3145	24.7	59.2	78	4970	3.5	0.840	3.5	3.68	41.2	0.162	0.36

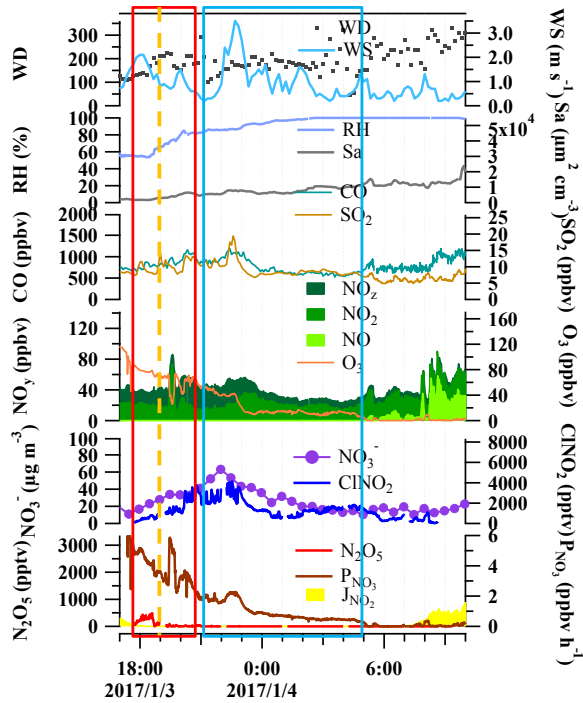


Figure 2. Variation of  $\text{N}_2\text{O}_5$ ,  $\text{ClNO}_2$ ,  $\text{NO}_3^-$ , trace gases and meteorological conditions during the nighttime of Jan 3 to 4, 2017.

The related texts in the original manuscript were also revised carefully. The following sentences were added.

Line 327: The data show that the uptake coefficient ranged from 0.009 to 0.066.

Line 331-335: It is interesting to see much higher  $\gamma_{\text{N}_2\text{O}_5}$  (0.066) on Jan 3 than those in other four nights (0.009-0.015), resulting from higher  $\text{P}_{\text{NO}_3}$  but much lower  $\text{Sa}$  and relatively low  $\text{N}_2\text{O}_5$  concentrations on Jan 3. We examined known factors affecting the loss of  $\text{NO}_3^-$  and  $\text{N}_2\text{O}_5$  such as the concentrations of  $\text{NO}$ , NMHCs and aerosol compositions, but found no obvious difference between Jan 3 and other nights.

Line 341-343: The correlation between  $\gamma_{\text{N}_2\text{O}_5}$ ,  $\phi_{\text{ClNO}_2}$  and the concentrations of aerosol compositions (see Table S2) or RH was investigated, and the results (not shown here) did not indicate any significant dependence of  $\gamma_{\text{N}_2\text{O}_5}$  or  $\phi_{\text{ClNO}_2}$  on these parameters.

*Minor comments:*

*The description of the experimental setup of the key relevant parameters needs to be*

strengthened, e.g. the limit of detection, the measurement uncertainties and measurement principle should be described.

Response: Table 1 with the limit of detection, the measurement uncertainties and measurement principle was added in the manuscript.

Table 1. Technique, limit of detection, and uncertainty of measuring instruments for trace gases and aerosols.

Species	Measurement techniques	Uncertainty	Detection limits
$\text{ClNO}_2, \text{N}_2\text{O}_5$	CIMS	$\pm 25\%$	6 pptv
HONO	LOPAP	$\pm 20\%$	7 pptv
$\text{O}_3$	UV photometry	$\pm 5\%$	0.5 ppbv
NO	Chemiluminescence	$\pm 20\%$	0.06 ppbv
$\text{NO}_2$	Photolytical converter & Chemiluminescence	$\pm 20\%$	0.3 ppbv
$\text{NO}_y$	MoO catalytic converter & Chemiluminescence	$\pm 5\%$	<0.1 ppbv
$\text{SO}_2$	Pulsed-UV fluorescence	$\pm 5\%$	0.1 ppbv
CO	IR photometry	$\pm 5\%$	4 ppbv
NMHCs	GC-FID/MS	$\pm 15\text{-}20\%$	20-300 pptv
OVOCs	DNPH-HPLC	$\pm 1\text{-}15\%$	20-450 pptv
$\text{PM}_{2.5}$	MAAP	$\pm 10\%$	$<0.1 \mu\text{g m}^{-3}$
Aerosol Ions	GAC-IC	$\pm 10\%$	$0.01\text{-}0.16 \mu\text{g m}^{-3}$
OC/EC	RT-4 SUNSET	$\pm 4\text{-}6\%$	$0.2 \mu\text{g cm}^{-2}$

Line 161. The reference of Yue et al., 2015 may not appropriate and suggests replacing by Dong et al., 2012 Dong, H. B., Zeng, L. M., Hu, M., Wu, Y. S., Zhang, Y. H., Slanina, J., Zheng, M., Wang, Z. F., and Jansen, R.: Technical Note: The application of an improved gas and aerosol collector for ambient air pollutants in China, *Atmos Chem Phys*, 12, 10519-10533, 10.5194/acp-12-10519-2012, 2012.

Response: The suggested reference was adopted.

Line 586 (figure 2) please check the data of wind speed, as the WS keep below  $3 \text{ m s}^{-1}$  during the whole half month. And the plot style of  $\text{NO}_y$  made the concentration of  $\text{NO}_2$  hard to follow. The left y-axis of fourth panel should change to  $\text{PM}_{2.5}$  or other more appropriate name.

Response: We did not find problem with the wind speed data, and the wind speed data shown in the figure was 10 min average. The very low wind speeds in the observation period were consistent with the regional meteorological conditions presented in the pressure contour in the weather chart. We also investigated the regional wind speed in PRD during this period from some websites and found that low wind speed was a regional phenomenon. Our personnel on site in fact felt little wind flow during the period. The figure below shows the wind speed (5 min average) from Dec 23, 2016 to Jan 20, 2017 at Heshan site, and the wind speed reached 7  $\text{m s}^{-1}$  before Jan 2017. Therefore, the low wind speeds were real and conducive to the occurrence of the severe haze.

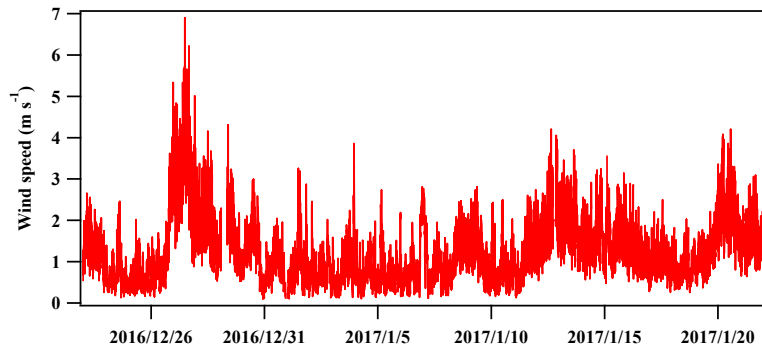


Figure 3. Wind speed from Dec 23, 2016 to Jan 20, 2017 at Heshan site.

The plot style of  $\text{NO}_y$ ,  $\text{NO}_2$  and  $\text{NO}$  was changed in the mentioned Figure. The left y-axis of fourth panel was changed to  $\text{PM}_{2.5}$ .

*The legend of the early night and later night in figure 6 and 7 should be explained. By the way, how about the  $\text{NO}_3^-$  formation potential intercomparison in the day and night of Jan 9 to 10.*

Response: The periods in the early nighttime in Fig.6 and Fig.7 correspond to the periods in Table 2 in the revised manuscript. And the periods in the later nighttime correspond to the periods in Table 3 in the revised manuscript. So the captions of Fig.6 and Fig.7 were changed to make them better understood. The comparison of the  $\text{NO}_3^-$  formation potential in the day and night of Jan 9 and 10 was not conducted due to the lack of data of NMHC after Jan 8 which made the model simulation of OH infeasible on the day of Jan 9. In the caption of Fig.7, the explanation was added as follows.

Line 680-684: Figure 6. Comparison between the measured  $\text{NO}_3^-$  increase and the  $\text{NO}_3^-$  formation potential in the early nighttime (periods in Table 2: Jan 3 17:40-19:00, Jan 4 17:00-22:00, Jan 5 17:00-22:00, Jan 6 17:00-22:40, Jan 9 19:00-00:20) and in the later nighttime (periods in Table 3: Jan 3-4 21:00-05:00, Jan 5 01:30-06:50, Jan 5-6 23:40-01:10, Jan 6-7 23:00-06:00, Jan 10 01:50-03:30).

Line 686-694: Figure 7. Comparison between the daytime (7:00 to 17:00 LT, assuming all gas phase  $\text{HNO}_3$  partitioned into particle phase) and nighttime (17:00 to 7:00 LT of the next day)  $\text{NO}_3^-$  formation potential. The early nighttime in each day represents the periods in Table 2, including Jan 3 17:40-19:00, Jan 4 17:00-22:00, Jan 5 17:00-22:00, Jan 6 17:00-22:40, and Jan 9 19:00-00:20. The later nighttime in each day represents the periods in Table 3, including Jan 3-4 21:00-05:00, Jan 5 01:30-06:50, Jan 5-6 23:40-01:10, Jan 6-7 23:00-06:00, and Jan 10 01:50-03:30. The intercomparison of the  $\text{NO}_3^-$  formation potential in the day and night of Jan 9 and 10 was not conducted due to the lack of data of NMHC after Jan 8 which made the model simulation of OH infeasible on the day of Jan 9.